

## NUMERICAL STUDY ON FLOW AND HEAT TRANSFER CHARACTERISTICS OF JET IMPINGEMENT

Xinjun Wang<sup>\*</sup>, Rui Liu, Xiaowei Bai, Jinling Yao

School of Energy and Power Engineering, Xi'an Jiaotong University, Xi'an 710049, China

### ABSTRACT

A mathematical model used for studying jet impingement cooling characteristics is established, and the rationality of the calculation model and method is confirmed by the experimental data. The CFX software is used to numerically simulate the jet impingement cooling characteristics on a gas turbine blade. The effects of various parameters, such as the arrays of impinging nozzles, the jet Reynolds number, the jet-to-jet distance, the ratio of nozzle-to-surface spacing to jet diameter  $H/d$ , and the radius of curvature of the target surface, on the flow and heat transfer characteristics of a impingement cooling process are studied. The results indicate that the impingement jets can make complex vortex in the cooling channel, the flow boundary layer is extremely thin and highly turbulent. Underneath each impingement nozzle, there will appear a low temperature area and a peak of Nusselt number on the impingement target surface, the distribution of temperature and Nusselt number on the target surface are associated with arrangement of impingement nozzles. The average Nusselt number of the in-line arrangement nozzles is higher than that of the staggered arrangement ones. With the increasing of jet Reynolds number, the velocity impinging on the target surface and Nusselt number increase. However, heat transfer of impingement cooling on target surface is not sensitive to the jet nozzles distance; the velocity impinging on the target surface and Nusselt number decrease with the increasing of the  $H/d$  value. For the curved target surface cases, the average Nusselt number of the target surface and the effect of heat transfer decreased with the increasing of curvature radius  $R$ .

*Key words:* turbine blade; impingement cooling; flow and heat transfer; numerical calculation.

### 1. INTRODUCTION

Current inlet temperature of advanced gas turbine is reached to 1500°C and the efficiency of single engine can be up to 39%. However, high gas temperature will bring high temperature corrosion to the turbine blades, especially at the blade leading edge where faces impingement of the high temperature flows

directly. Therefore, the effective cooling should be applied to protect the turbine blades<sup>[1-2]</sup>.

Jet impingement is the most effective way to enhance local heat transfer coefficient. Impingement cooling indicates that the cooling medium impinges on the high temperature solid wall at high speed, brings the heat away from solid wall, and protects high temperature components. The impingement cooling is used when the thermal load is significant high. The leading edge of turbine blade bears the highest thermal load and the cross-section of blades is thicker, so the jet structure should be applied. In addition, the strength requirement of stator blades is lower than rotor blades, so jet impingement cooling is also applied in the middle portion of stator blades.

The blade leading edge of gas turbine is curving, and the curved impingement target surface affects the flow and heat transfer characteristic of impingement cooling. In the middle portion of blades, the ratio of curvature radius of the target surface to jet diameter is larger. The target plane is usually assumed in the vertical direction of jet impingement. Moreover, due to scattered jet flow, the transverse flow will change the flow and heat transfer characteristics of neighbor jets. Meanwhile, transverse flow may be produced by impingement cooling in the blade leading edge and then affects the impingement cooling in the middle portion area. Therefore, the transverse flow is initial transverse flow, and will significantly affect the flow boundary layer and distribution of mass in the jet row<sup>[3-4]</sup>.

Many studies on the jet impingement cooling have been developed<sup>[5-14]</sup>. Jambunathan et al. [9] collated and critically reviewed heat transfer data for single circular jet impingement. Martin [10] studied heat and mass transfer between impinging gas jets and solid surfaces. Popiel and Trass [11] observed the behavior of natural free and impinging round at low nozzle-to-plate separations. Goldstein and Timmers [14] applied a visualization technique to measure the heat transfer coefficient distribution on a flat plate on which either a single jet or an array of jets impinges. Their result showed that with multiple jets, flow interaction could cause the mixing-induced turbulence to penetrate further towards the center of individual jets. Viskanta

[13] studied heat transfer characteristics of single and multiple isothermal turbulent air and flame jets impinging on surfaces. Both circular and slot two-dimensional jets were considered, and the effect of crossflow on impingement heat transfer was included. Gau and Chung [12] investigated the effect of surface curvature on the structure of an impinging jet flow. They found that in the case of impingement cooling on a concave surface, the local Nusselt number increases with increasing surface curvature.

In this paper, ANSYS-CFX software is applied to numerical study the jet impingement cooling characteristics of the leading edge and middle portion area of blade. The effects of the cooling structure and flow parameters on the flow and heat transfer characteristics of impingement cooling are discussed.

## 2.GOVERNING EQUATIONS AND TURBULENT MODEL

### 2.1 Governing Equations

In the rectangular coordinate system  $(i, j, k)$ , the differential form of continuity equation, momentum equation and energy equation can be expressed as follows:

$$\frac{\partial \rho}{\partial t} + \nabla \cdot (\rho \vec{U}) = 0 \quad (1)$$

$$\frac{\partial (\rho \vec{U})}{\partial t} + \nabla \cdot (\rho \vec{U} \otimes \vec{U}) = \nabla \cdot (-p \delta + \mu (\nabla \vec{U} + (\nabla \vec{U})^T)) + S_M \quad (2)$$

$$\frac{\partial (\rho h^*)}{\partial t} - \frac{\partial p}{\partial t} + \nabla \cdot (\rho \vec{U} h^*) = \quad (3)$$

$$\nabla \cdot (\lambda \nabla T) + \nabla \cdot (\mu \nabla \vec{U} + \nabla \vec{U}^T - \frac{2}{3} \nabla \cdot \vec{U} \delta \vec{U}) + S_E$$

Here  $S_M$  is momentum source,  $S_E$  is energy source and  $h^*$  is ratio of total enthalpy.

The definitions of Reynolds number  $Re$ , local heat transfer coefficient  $h$ , the local Nusselt number  $Nu$  and the average Nusselt number  $Nu_0$  are as follows:

$$Re = \frac{ud}{\nu}, h = \frac{q}{T_w - T_j}, Nu = \frac{hd}{\lambda_j}, Nu_0 = \frac{h_0 d}{\lambda_j} \quad (4)$$

Here  $u$  is jet velocity,  $d$  is diameter of jet nozzles,  $\nu$  is kinematic viscosity,  $q$  is heat flux density of impingement target surface,  $T_w$  is target wall temperature,  $T_j$  is jet temperature at the inlet of impingement nozzle,  $h$  is local heat transfer coefficient of target surface,  $h_0$  is average heat transfer coefficient and  $\lambda_j$  is heat conduction coefficient of cooling medium.

### 2.2 Mesh Density and Selection of Turbulent Model

San et al. [15] performed a measurement of the local Nusselt number of a confined circular jet vertically impinging on a plate. The recirculation and mixing effect on the heat transfer is investigated by varying the jet diameter, surface heat flux Reynolds number and surface heating width. Based on the

experimental data of San, this paper numerical performs the effects of mesh density and turbulent model on calculation results accuracy. The calculation model and boundary conditions are the same as the experimental conditions of San. The structured mesh is adopted and the number of mesh is 1 million, 1.2 million, 1.5 million and 2.2 million respectively. The space between the first node and the wall surface is 0.0001 mm (the value of  $Y^+$  is 5), grid density is 1.2. Five turbulent models (SST, SST- $\gamma$ , SST- $\gamma$ - $\theta$ ,  $\kappa$ - $\epsilon$  and  $\kappa$ - $\omega$ ) are selected.

Fig.1 and Fig.2 show the effects of mesh number and turbulent model on distribution of local Nusselt number on the target surface in the single-nozzle jet impingement. And  $x$  in Fig.1 and Fig.2 indicate the distance of in the direction of  $x$  axis,  $Nu$  and  $Nu/Re^{0.6375}$  are used to indicate the effect of heat transfer. The results show that with the increasing of mesh number, the calculation Nusselt number decreases and approaches experimental data gradually; when the mesh number is more than 1.5 million, the mesh number affects calculation results slightly. In the five turbulent models, the calculation applied SST model have closest results with experimental data. Therefore, 1.5 million mesh number and SST turbulent model are chosen to calculate the impingement cooling characteristics.

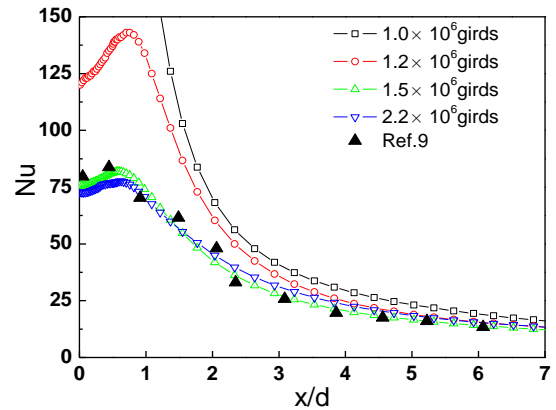


Fig.1 Effect of mesh number on local Nusselt number

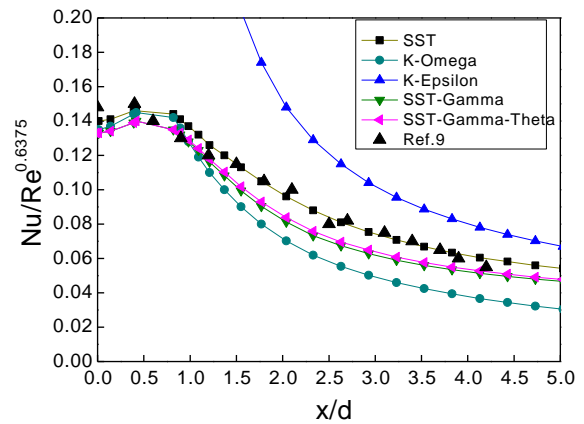
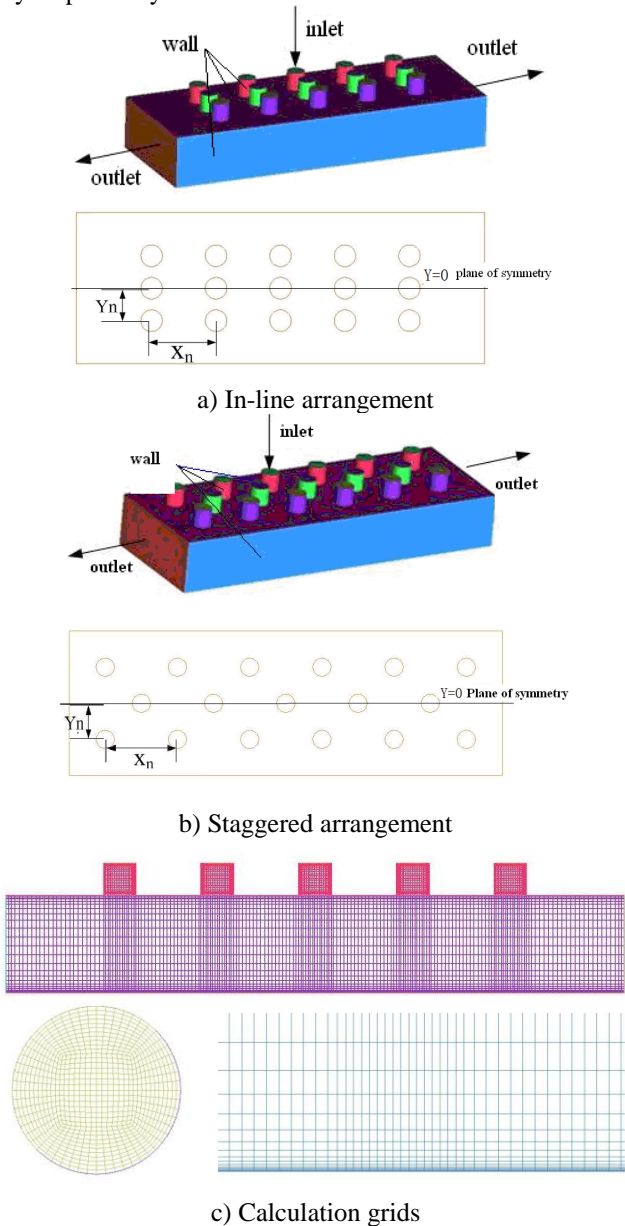


Fig.2 Effect of turbulent model on local Nusselt number

### 3. FLOW AND HEAT TRANSFER OF IMPINGEMENT COOLING IN MIDDLE PORTION OF BLADE

In the gas turbine blade, the jet impingement of multi-row nozzles is applied. At the middle portion of blade, the target plane of impingement cooling is usually assumed in the vertical direction of jet impingement. Calculation model and grids of the middle portion of the blade are shown in Fig.3. In-line and staggered arrangement are adopted respectively.  $X_n$  and  $Y_n$  indicate the distance of impingement jets in the direction of  $x$  and  $y$  respectively.



**Fig.3 Calculation model and grids for the middle portion of blade**

The cooling medium is air, the diameter of impingement nozzles  $d$  is 4mm; the ratio of distance from impingement

nozzles to target surface  $H$  to nozzle's diameter is  $H/d=3$ ; jet Reynolds number  $Re$  is 5000、10000、15000 respectively; the solid boundary is assumed as adiabatic and no slipping; the inlet air temperature  $T_{in}$  is set as 303K and the direction of velocity is normal; outlet is set as static pressure; impingement target surface is set as constant heat flux density  $q=3000W/m^2$ . The SST turbulent model and structured grid are selected. The equations are discretized using a second-order accurate upwind finite volume scheme. And the convergence criterion is that the root means square residuals of both pressure and velocity components in three directions are less than  $1 \times 10^{-5}$ .

#### 3.1 The Effect of In-line And Staggered Arrangement

The case of  $X_n=8d$ ,  $Y_n=4d$  was discussed. Fig.4 shows streamline of cooling air on the  $Y=0$  plane of symmetry in both the in-line and staggered arrangements. Whether in in-line or staggered case, cooling air from impingement nozzles impinges on target surface and generates a stagnation zone under the impingement nozzles, the flow velocity in stagnation zone is 0. Because of interaction between each jet, the complex vortex is produced in the cooling channel. The thin and highly turbulent boundary layer in the jet impingement area and its nearby area can significantly strengthen the heat transfer process. In general, transverse flow has little influence on the middle jets, the middle jets is similar to the single impingement jet; however, two impingement near the outlet are significantly affected by the transverse flow, jets flow are deflected to outlet.

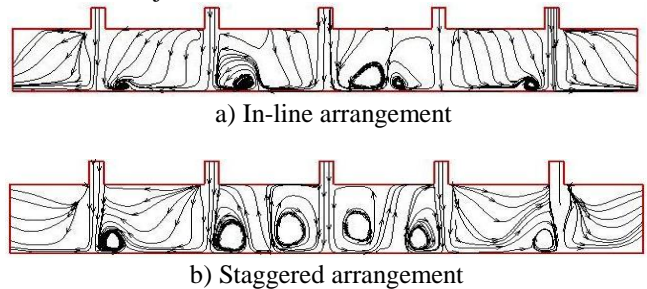
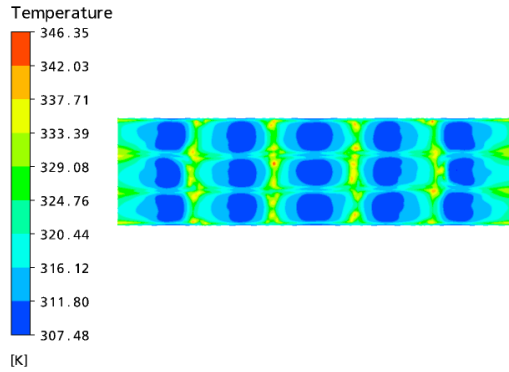
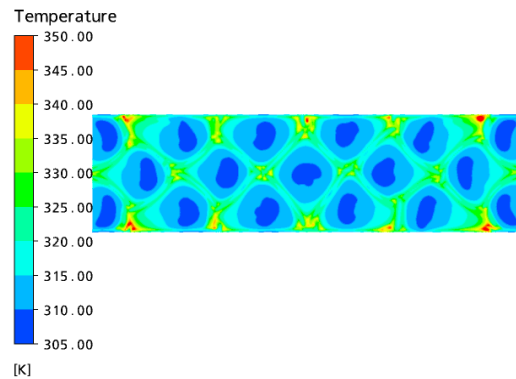


**Fig.4 Streamline at  $Y=0$  symmetry plane when  $Re=10000$**

Fig.5 and Fig.6 show distribution of temperature and Nusselt number on the impingement target surfaces in the in-line and staggered arrangement cases, respectively. In the two arrangements, corresponding to each impingement nozzle there will appear a low temperature area and a peak of  $Nu$  in the target surface. In the middle area, the transverse flow affects heat transfer slightly, the distribution of temperature and Nusselt number is symmetrical, but near the both left and right outlet, the influence of transverse flow on heat transfer is significant, and the flow shows unsymmetrical in distribution of temperature and Nusselt number. In general, the distribution of temperature and Nusselt number on the target surface is associated with arrangement of impingement nozzles, the average Nusselt number in the in-line arrangement cases are higher than the staggered arrangement ones.

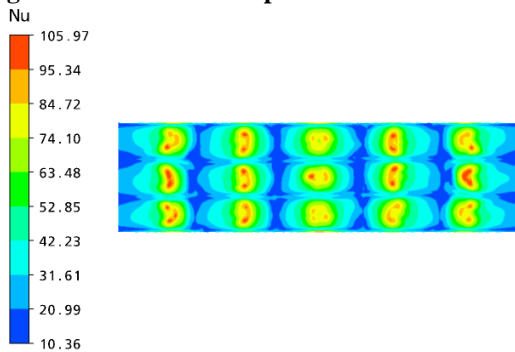


a) In-line arrangement

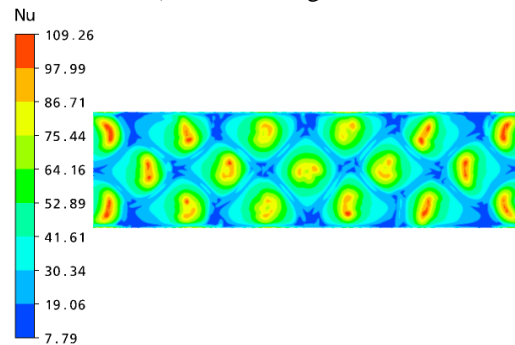


b) Staggered arrangement

**Fig.5 Distribution of temperature when Re=10000**



a) In-line arrangement



b) Staggered arrangement

**Fig.6 Distribution of Nusselt number when Re=10000**

### 3.2 The Influence of Jet Reynolds number

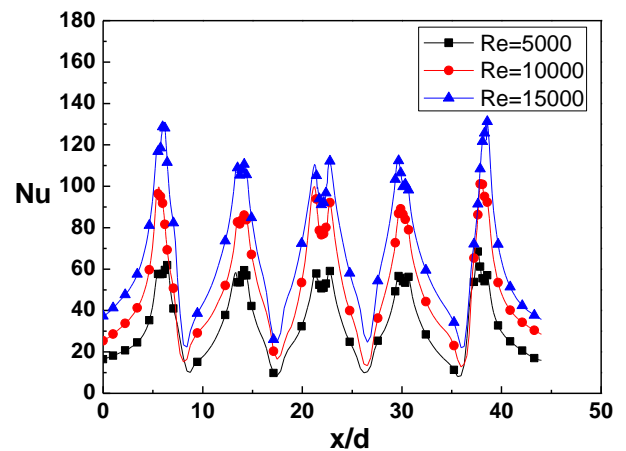
Fig.7 shows the distribution of local Nusselt number on the intersecting line between  $Y=0$  symmetry plane and target surface both in in-line and staggered arrangement cases. And  $x=0$  in Fig.7 is at the location of left outlet. With the increasing of jet Reynolds number, the velocity of impinging on target surface increases and flow near the target surface is strengthened, which enhances the convective heat transfer between fluid and target surface, the decreasing of target surface temperature and the increasing of Nusselt number will appear. When the inlet Re increases from 5000 to 15000, the highest temperature of target surface in the in-line arrangement cases decreases from 373K to 336K and the highest Nu increases from 70 to 138; the highest temperature in the staggered arrangement cases decreases from 390K to 335K and the highest local Nusselt number increases from 70 to 141.

### 3.3 The Influence of Jet Nozzles Distance

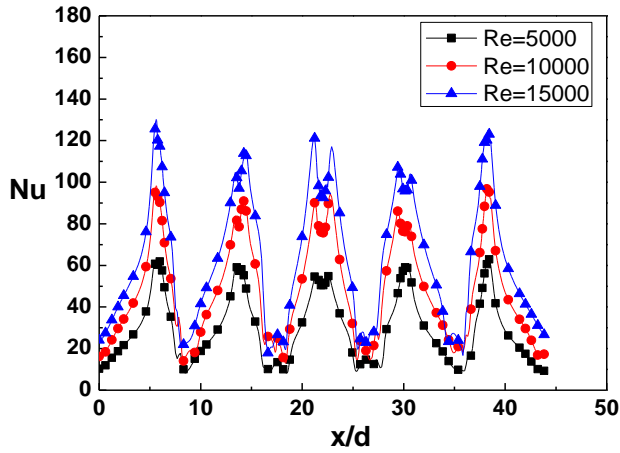
Table1 gives three kinds of parameter combination about jet nozzles distance. Fig.8 is under three kinds of distance, the average Nusselt number on impingement target surface in both in-line and staggered arrangement cases. For in-line arrangement, the average Nusselt number of structure 3 is higher than the other structures; for staggered arrangement, the average Nusselt number of structure 2 is higher. In general, heat transfer of impingement cooling on target surface is not sensitive to the jet nozzles distance.

**Table1 Parameter combination of three kinds of jet nozzles distance**

	in-line arrangement	staggered arrangement
structure 1	$X_n=8.0d; Y_n=4.0d$	$X_n=8.0d; Y_n=4.0d$
structure 2	$X_n=4.0d; Y_n=2.0d$	$X_n=4.0d; Y_n=2.0d$
structure 3	$X_n=3.0d; Y_n=1.5d$	$X_n=3.0d; Y_n=1.5d$

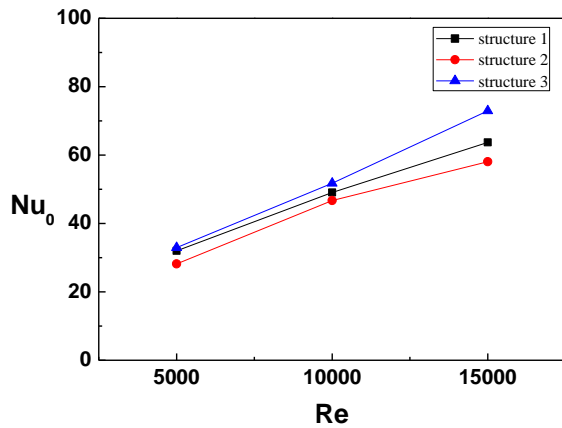


a) In-line arrangement

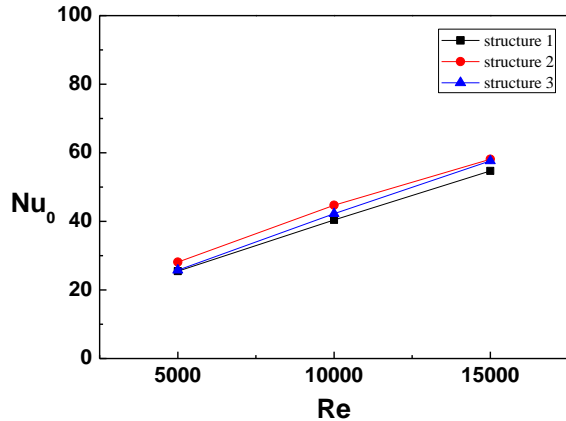


b) Staggered arrangement

**Fig.7 Distribution of Nu on intersecting line between Y=0 symmetry plane and target surface**



a) In-line arrangement



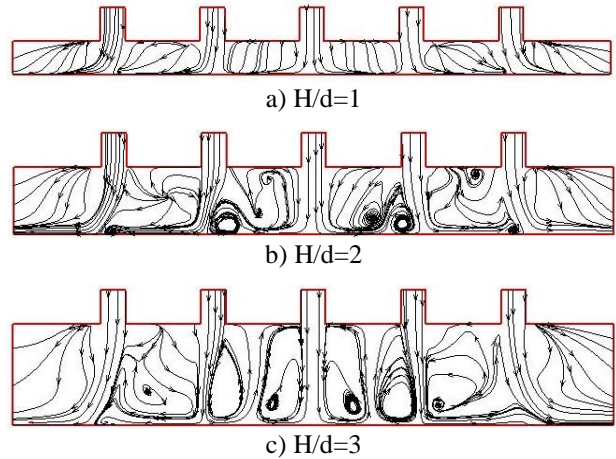
b) Staggered arrangement

**Fig.8 The average Nusselt number on impingement target surface**

### 3.4 The Influence of H/d

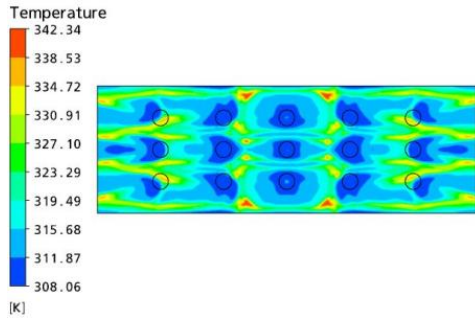
In the middle portion of typical gas turbine, the value of  $H/d$  is 1~3. For the  $X_n=4d$ ,  $Y_n=2d$ ,  $Re=5000$ , in-line arrangement, the flow and heat transfer characteristics of multi-row nozzles jet impingement are studied for three situations ( $H/d=1$ ,  $H/d=2$ ,  $H/d=3$ ).

Fig.9 gives the streamline distributions on  $Y=0$  symmetry plane. It shows that: ① jet impinges from impingement nozzles to target surface create stagnation zones under the impingement nozzles. The middle jets have the similar features of single impingement jet, two impingement nozzles near outlet are significantly affected by transverse flow and the jets are deflect to outlet. ② when  $H/d$  is smaller, because of limitation of flow space and the influence of nearby jets, jet flow don't produce significant vortex in  $Y=0$  symmetry plane; when  $H/d$  is larger, flow space increases, restrictive effect of solid boundary on flow weakens. Many complex vortexes are created in  $Y=0$  plane.

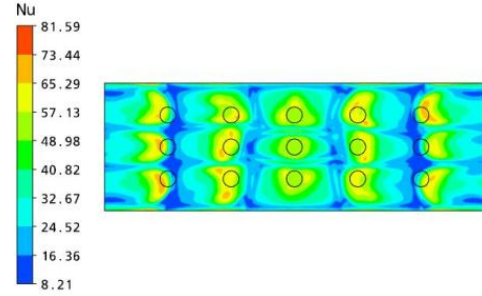


**Fig.9 Streamline on symmetry plane of different H/d (in-line arrangement)**

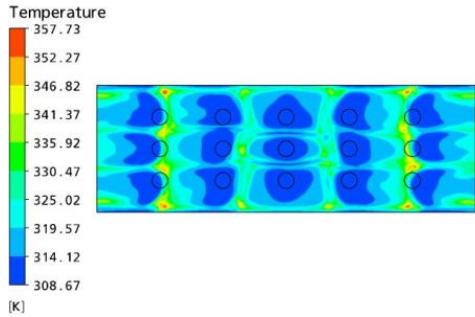
In three different kinds of  $H/d$ , the distributions of temperature and Nusselt number on impingement target surface are shown in Fig.10 and Fig.11 respectively. The circles indicate position of impingement nozzles. Corresponding to each impingement nozzle, there will appear a low temperature area on the target surface and local Nusselt number is peak, the minimum of temperature and the peak of local Nusselt number appear just under impingement nozzles. With the increasing of  $H/d$ , velocity impinging on target surface decreases, the flow near target surface becomes slower, so the convective heat transfer between the flow and target surface is weakened. Therefore, the temperature of target surface becomes higher,  $Nu$  becomes lower. When  $H/d$  increases from 1 to 3, the highest temperature in target surface increases from 342K to 360K, the highest local Nusselt number decreases from 92 to 77. Fig.12 is effect of  $H/d$  on the average Nusselt number on the target surface.



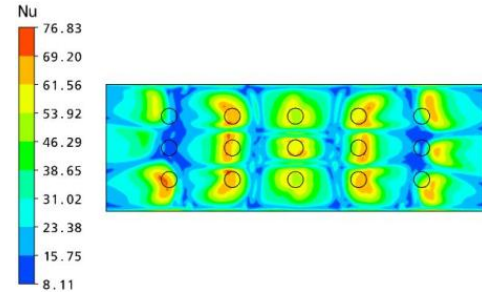
a)  $H/d=1$



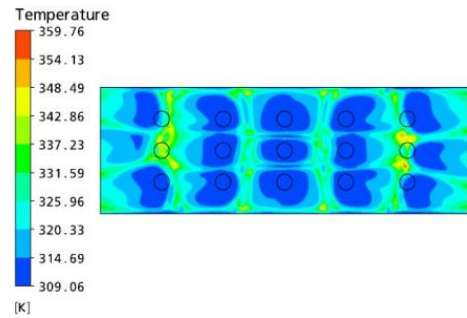
b)  $H/d=2$



b)  $H/d=2$

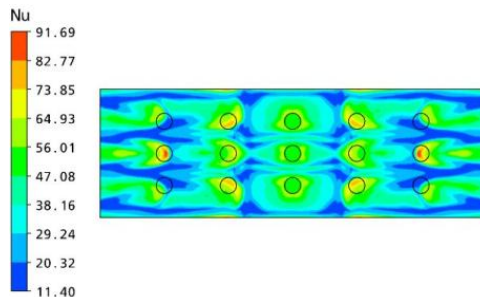


c)  $H/d=3$



c)  $H/d=3$

**Fig.10 Distribution of temperature on impingement target surface**



a)  $H/d=1$

**Fig.11 Distribution of Nu on impingement target surface**

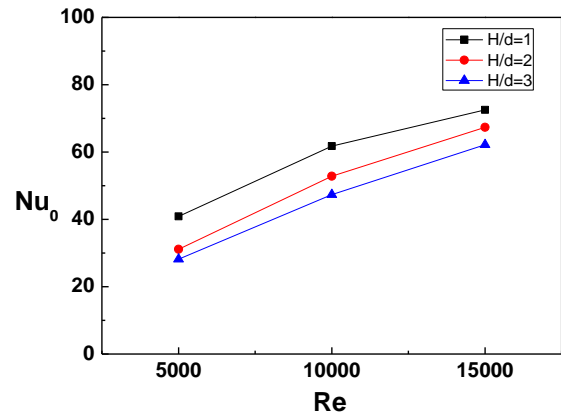


**Fig.12 Effects of  $H/d$  on the average Nusselt number on impingement target surface**

#### 4. FLOW AND HEAT TRANSFER OF IMPINGEMENT JETS IN THE LEADING EDGE

The leading edge of gas turbine blade bears the highest thermal load, and needs to arrange impingement cooling. However, the leading edge of the blade is curving, so impingement target surface is curved. Fig.13 shows the calculation model and grids for leading edge. The structure of single-row five nozzles is applied and jets discharge from two sides. Diameter of impingement nozzles is 4mm; the cooling medium is air, solid boundary is assumed as adiabatic and no slipping; the inlet air temperature  $T_{in}$  is 303K, outlet is set as static pressure; impingement target surface is set as constant heat flux density  $q=5000W/m^2$ . The SST turbulent model is applied. The equations are discretized using a second-order accurate

upwind finite volume scheme. The convergence criterion is that the root means square residuals of both pressure and velocity components in three directions are less than  $1 \times 10^{-5}$ .

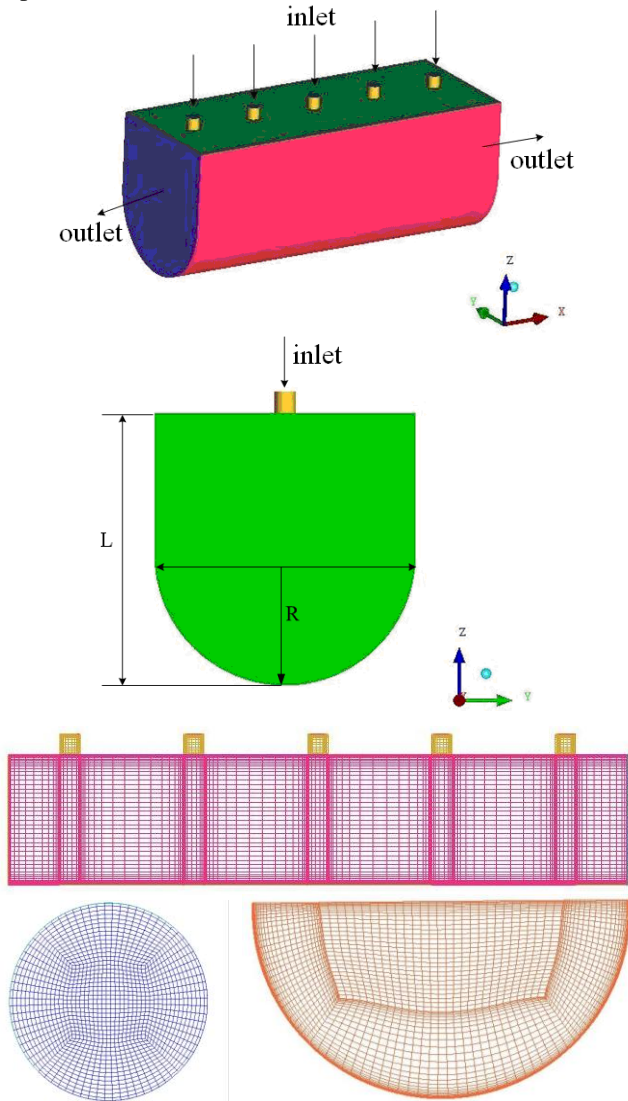
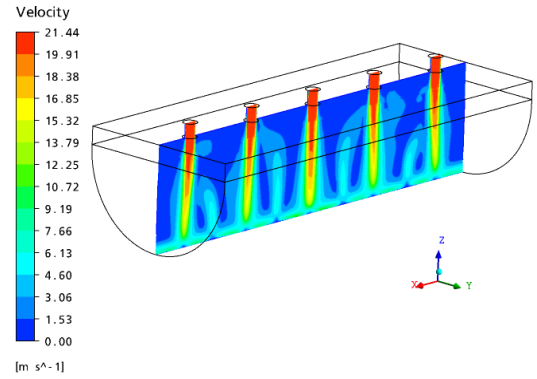


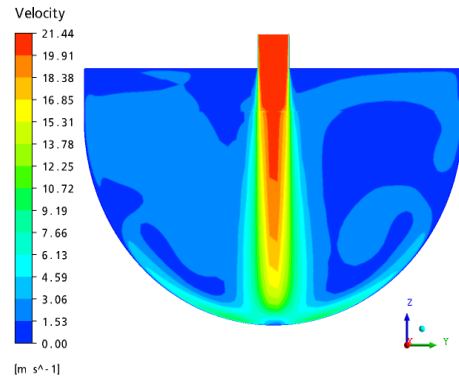
**Fig.13 Calculation model and grids for the leading edge of blade**

#### 4.1 The Influence of L

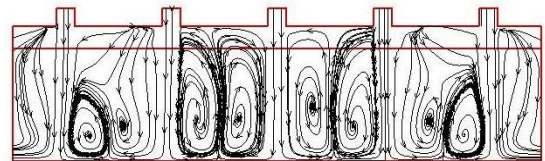
Fig.14 illustrates the velocity and streamline on the XZ plane and YZ plane under conditions of  $R=25\text{mm}$  and  $L=30\text{mm}$ . Jets impinge on curved target surface and generate stagnation zones under the impingement nozzles; due to interaction among jets, the complex vortexes are created on the XZ plane (Fig.14a and Fig.14c), and two symmetrical vortexes are formed on the YZ plane (Fig.14b and Fig.14d).



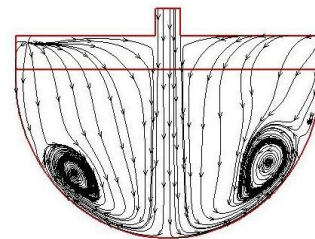
a) Velocity on XZ plane



b) velocity on YZ plane



c) Streamline on XZ plane

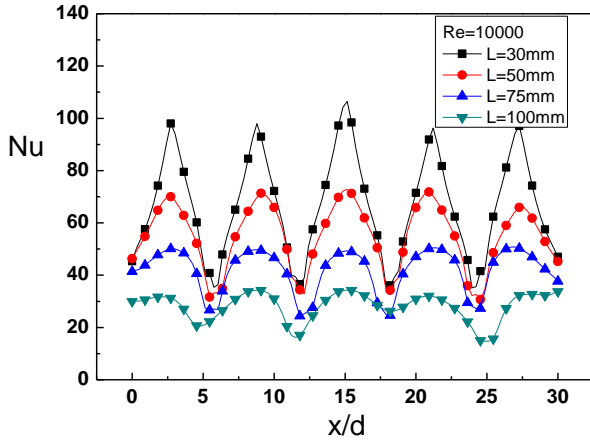


d) Streamline on YZ plane

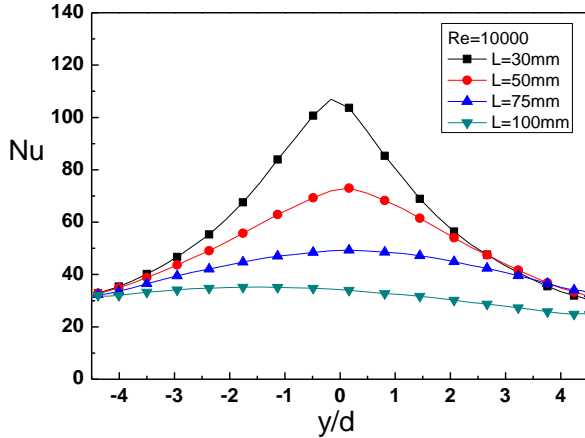
**Fig.14 Distribution of velocity and streamline on the XZ plane and YZ plane**

Fig.15 illustrates distribution of Nu on the intersecting line among XZ plane, YZ plane and target surface under the conditions of  $R=25\text{mm}$  and  $Re=10000$  respectively. With the increasing of L, local Nusselt number on the target surface becomes lower. While L increases from 30mm to 100mm, the highest local Nusselt number on the target surface decreases from 62 to 24. When L is lower (such as  $L=30\text{mm}$  and  $50\text{mm}$ ),

the influence of transverse flow is weakened, the peak of Nu is vertically underneath the impingement nozzle; when L is larger (such as L=75mm and 100mm), the influence of transverse flow is enhanced, the peak of Nu deviates from vertically subjacent position of impingement nozzles.



a) Nu distribution on intersecting line between XZ plane and target surface

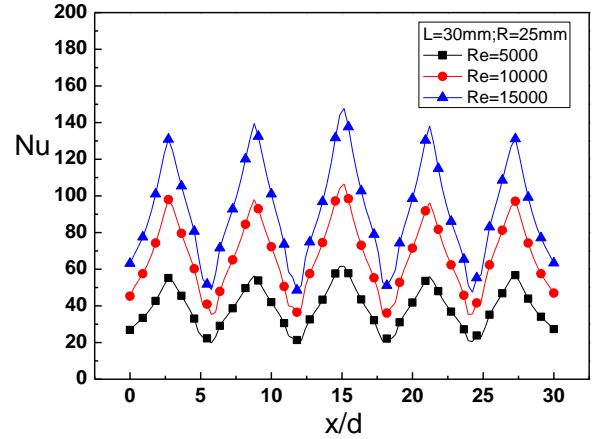


b) Nu distribution on intersecting line between YZ plane and target surface

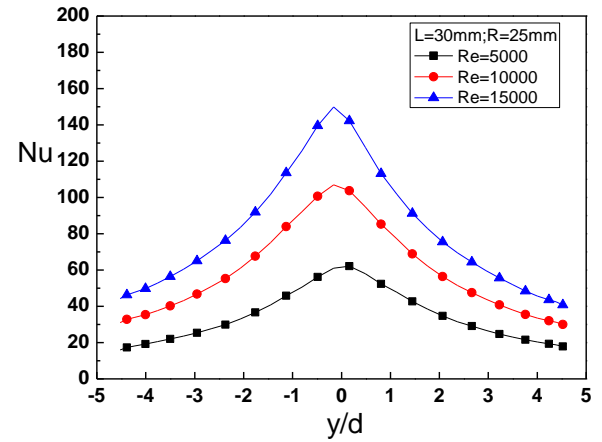
**Fig.15 Effect of L on the local Nusselt number distribution when Re=10000**

#### 4.2 The Influence of Jet Reynolds number

Fig.16 shows the effect of jet Reynolds number on the local Nusselt distribution at the target surface under the conditions of L=30mm and R=25mm. With the increasing of Re, the velocity impinging on the target surface is enhanced, flow near the target surface is strengthened, the temperature on target surface becomes lower and Nusselt number becomes higher. The highest local Nusselt number on target surface increases from 62 to 151, while Re increases from 5000 to 15000.



a) Distribution of Nu on the intersecting line between XZ plane and target surface



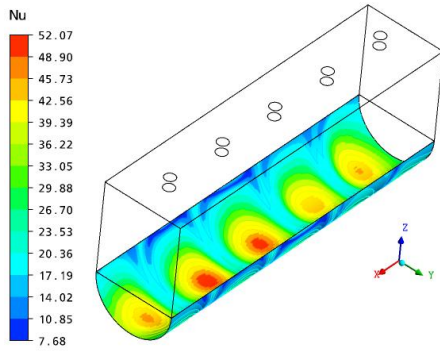
b) Distribution of Nu on the intersecting line between YZ plane and target surface

**Fig.16 Effect of Re on distribution of the local Nusselt number**

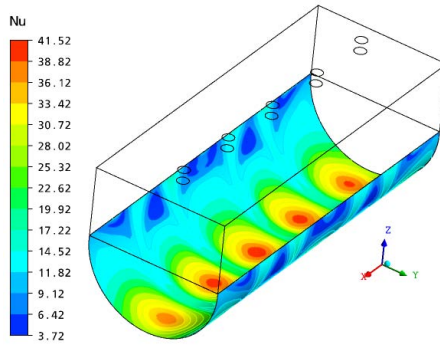
#### 4.3 The Influence of Curvature Radius of Target Surface

Fig.17 presents the effect of curvature radius R on Nusselt number distribution on impingement target surface under the condition of Re=10000, L=50 mm, d=4mm. Fig.18 shows the local Nusselt number distribution on the intersecting line among XZ plane, YZ plane and target surface. With the increasing of curvature radius R, Nu on the target surface gradually decreases. While curvature radius R increases from 15mm to 40mm, the highest local Nusselt number on the target surface decreases from 52 to 38.

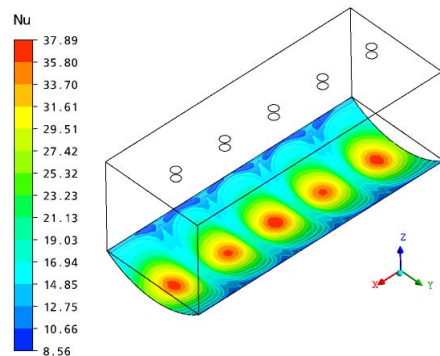
Fig.19 is the effect of curvature radius on average Nusselt number of impingement target surface in three kinds of jet Reynolds numbers. With the increasing of curvature radius R, average Nusselt number gradually decreases; when impingement target surface is a plane, the value of  $Nu_0$  is lowest, and the heat transfer effect is worst.



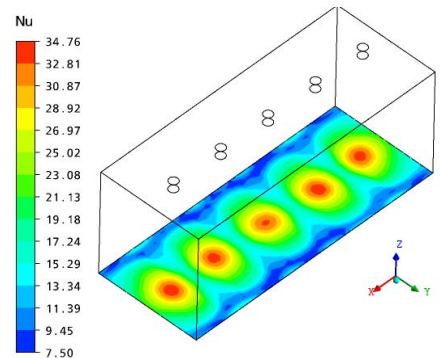
a) R=15mm



b) R=25mm

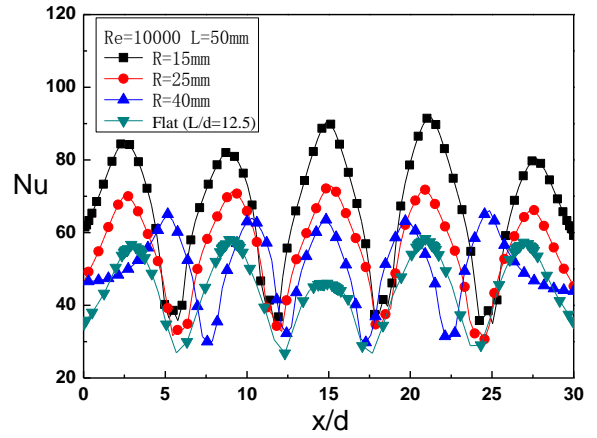


c) R=40mm

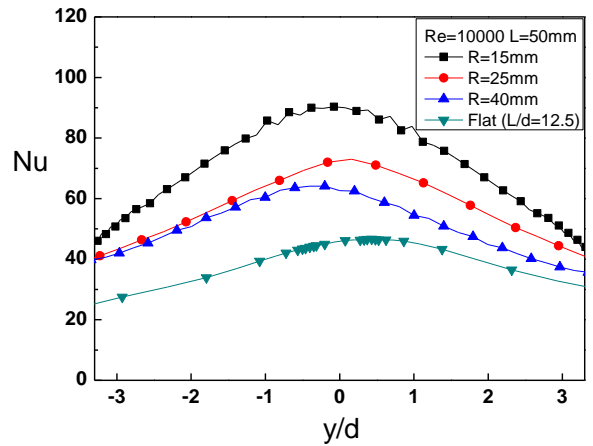


d) Plane surface

**Fig.17 Nu distribution on target surface under different curvature radius**



a) Nu distribution in the X direction



b) Nu distribution on the intersecting line between YZ plane and target surface

**Fig.18 The local Nusselt number distribution with different R when Re=10000**

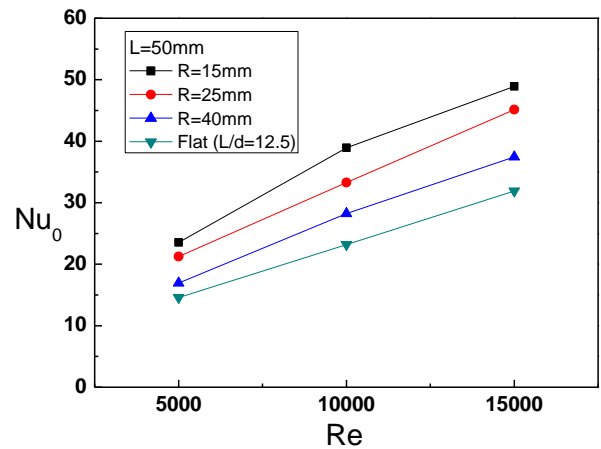


**Fig.19 Effect of curvature radius on the average Nusselt number of impingement target surface**

## 5. CONCLUSIONS

1) In the process of multi-row nozzles jet impingement, whether in-line arrangement or staggered arrangement, cooling air impinging from impingement nozzles to impingement target surface and generated a stagnation zone under the impingement nozzles; the interacted jets of each impingement nozzle would create complex vortex in cooling channel. The boundary layer of flow was very thin and highly turbulent; corresponding to each impingement nozzle there would appear a low temperature area and existed a peak of Nusselt number in the impingement target surface; the distribution of temperature and Nusselt number on the target surface was associated with arrangement of impingement nozzles; the average Nusselt number in the in-line arrangement was higher than the staggered arrangement.

2) With the increasing of jet Reynolds number, the impinging velocity increases, flow near target surface is strengthened, which enhanced the convective heat transfer between flow and target surface, so the Nusselt number increased; with the increasing of  $H/d$ , the velocity impinging the target surface decreased, flow near the target surface is weakened, so the convective heat transfer between flow and target surface was weakened, the temperature of target surface became higher and the value of Nusselt number became smaller.

3) In the curved target surface cases, the average Nusselt number on the target surface and the effect of heat transfer decreased with the increasing curvature radius  $R$ .

## ACKNOWLEDGMENTS

The research was supported by National Program on Key Basic Research Project (973Program) (No. 2007CB707701).

## NOMENCLATURE

$d$	diameter of jet nozzles
$h$	local heat transfer coefficient
$h_0$	average heat transfer coefficient
$q$	heat flux density of impingement target surface
$u$	jet velocity
$\nu$	kinematic viscosity
$H$	nozzle-to-plane spacing
$L$	nozzle-to-concave surface spacing
$R$	radius of curvature
$Nu$	local Nusselt number
$Nu_0$	average Nusselt number
$Re$	jet Reynolds number
$S_M$	momentum source
$S_E$	energy source
$h^*$	ratio of total enthalpy
$T_w$	target wall temperature
$T_j$	inlet temperature of impingement nozzle
$X_n$	distance of impingement jets in the direction of $x$
$Y_n$	distance of impingement jets in the direction of $y$
$\lambda_j$	heat conduction coefficient of cooling medium

## REFERENCES

- [1] Goldstein, R.J., Seol, W.S., 1991, "Heat transfer to a row of impinging circular air jets including the effect of entrainment." *International Journal of Heat and Mass Transfer*, 34: 2133-2147.
- [2] Goldstein, R.J., Sobolik, K.A., Seol, W.S., 1990, "Effect of entrainment on the heat transfer to a heated circular air jet impinging on a flat surface." *ASME Journal of Heat Transfer*, 112: 608-611.
- [3] Florschuetz, L.W., Su, C.C., 1987, "Effect of crossflow temperature on heat transfer within an array of impinging jets." *ASME Journal of Heat Transfer*, 106: 34-41.
- [4] Huang, Y.Z., Ekkad, S.V. and Han, J.C., 1998, "Detailed Heat Transfer Distributions under an Array of Orthogonal Impinging Jets." *Journal of Thermophysics and Heat Transfer*, 25: 73-79.
- [5] Huang, Y.Z., Ekkad, S.V. and Han, J.C., 1998, "Detailed Heat Transfer Distributions under an Array of Orthogonal Impinging Jets." *Journal of Thermophysics and Heat Transfer*, 12: 73-79.
- [6] Akella, K.V. and Han, J.C., 1998, "Impingement Cooling in Rotating Two-Pass Rectangular Channels." *AIAA Journal of Thermophysics and Heat Transfer*, 12(4): 582-588.
- [7] Akella, K.V. and Han, J.C., 1999, "Impingement Cooling in Rotating Two-Pass Rectangular Channels with Ribbed Walls." *AIAA Journal of Thermophysics and Heat Transfer*, 13(3): 364-371.
- [8] Garg, V. K. and Gaugler, R.E., 1997, "Effect of Coolant Temperature and Mass Flow on Film Cooling of Turbine Blades." *ASME Paper 95-WA/HT-1*. *International journal of heat and mass transfer*, 40(2): 435-444.
- [9] Jambunatham, K., Lai, E., Moss, M.A., Button, B. L., 1992, "A Review of Heat Transfer Data for Single Circular Jet Impingement." *Int. J. Heat Fluid Flow*, 13(2):106-115.
- [10] Martin, H., 1977, "Heat and Mass Transfer between Impinging Gas Jet and Solid Surfaces." *Advances in Heat Transfer*, 13:1-60.
- [11] Popiel, C.O. and Trass, O., 1991, "Visualization of a Free and Impinging Round Jet." *Experimental Thermal and Fluid Science*, 4:253-264.
- [12] Gau, C. and Chung, C. M., 1991, "Surface Curvature Effect on Slot-Air-Jet Impingement Cooling Flow and Heat Transfer Process." *ASME, Journal of Heat Transfer*, 113(4):858-864.
- [13] Viskanta, R., 1993, "Heat Transfer to Impinging Isothermal Gas and Flames Jets." *Exp. Thermal Fluid Sci*, 6: 111-134.
- [14] Goldstein, R.J. and Timmers, J. F., 1982, "Visualization of Heat Transfer from Arrays of Impinging Jets." *International Journal of Heat and Mass Transfer*, 25:1857-1868.
- [15] San, J.Y., Huang, C.H. and Shu, M.H., 1997, "Impingement cooling of a confined circular air jet." *International journal of heat and mass Transfer*, 40(6): 1355-1364.